

## BEAM LOSS STUDIES IN HIGH-INTENSITY HEAVY-ION LINACS \*

P. N. Ostroumov, V.N. Aseev, E.S. Lessner, B. Mustapha, Physics Division  
Argonne National Laboratory, 9700 S. Cass Avenue, Argonne, IL ,60439

### *Abstract*

A low beam-loss budget is an essential requirement for high-intensity machines and represents one of their major design challenges. In a high-intensity heavy-ion machine, losses are required to be below 1 W/m for hands-on-maintenance. The driver linac of the Rare Isotope Accelerator (RIA) is designed to accelerate beams of any ion to energies from 400 MeV per nucleon for uranium up to 950 MeV for protons with a beam power of up to 400 kW. The high intensity of the heaviest ions is achieved by acceleration of multiple-charge-state beams, which requires a careful beam dynamics optimization to minimize effective emittance growth and beam halo formation. For beam loss simulation purposes, large number of particles must be tracked through the linac. Therefore the computer code TRACK [1] has been parallelized. Calculations are being performed on the JAZZ cluster [2] recently inaugurated at ANL. This paper discusses how this powerful tool is being used for simulations for the RIA project to help decide on the high-performance and cost-effective design of the driver linac.

### SIMULATION CODE

A new beam-dynamics-simulation code, TRACK, has been developed and used for beam-loss studies in the RIA driver linac. Currently, the code supports practically all known electro-magnetic elements for acceleration, transport, and focusing of multi-component ion beams. In the code, ions are tracked through the three-dimensional electromagnetic fields of every element of the linac, starting from the ECR (Electron Cyclotron Resonance) ion source to the production target. The simulation starts with a multi-component DC ion beam extracted from the ECR. Space-charge forces are especially important in the front end of the driver linac and are included in the simulations. Beam losses are studied by tracking a large number of particles (up to  $10^6$ ) through the whole linac, considering a comprehensive set of sources of errors, such as element misalignments, RF-field errors and stripper-thickness fluctuations. For each configuration of the linac, multiple sets of error values have been randomly generated and used in the calculations. The results are then combined to calculate important beam parameters, estimate beam losses, and characterize the corresponding linac configuration.

The structure of the TRACK code and its ideology is close to the RAYTRACE code [3] except that TRACK has many additional features and capabilities. Unlike

RAYTRACE, TRACK integrates the equations of motion of all tracked particles in short distance intervals and calculates space-charge fields.

Space-charge fields of multi-component ion beams are solved with the Poisson equation [4]. The code calculates both two-dimensional (for DC beams) and three-dimensional (for bunched beams) space-charge fields. The three-dimensional Poisson equation is solved with rectangular boundary conditions in the transverse direction and periodic conditions along the direction of the beam propagation. A special routine has been written for the integration of multi-component DC ion beams through bending magnets.

Stripper effects on the particle distribution in phase space have been initially simulated using the SRIM code [5]. To incorporate the SRIM results into TRACK, a special parameterization procedure [6] has been developed. It takes into account the correlation of the energy loss and the scattering angle distributions. The procedure also includes the possibility to simulate fluctuations in the stripping foil thickness.

### BEAM DYNAMICS IN THE RIA DRIVER LINAC

A detailed configuration of the 1.4-GV RIA driver linac was described in ref. [7]. The linac consists of a front-end and three sections of SC linac: low-, medium- and high- $\beta$  sections. The front-end includes an ECR ion source, a low energy beam transport (LEBT) system, a multi-harmonic buncher (MHB), a radio frequency quadrupole (RFQ) and a medium energy beam transport (MEBT) system. The three sections of the linac are separated by two stripper areas, each with a stripper foil or film and a post-stripper magnetic transport system (MTS). Two options of the driver linac have been proposed. The first option is the elliptical cavity linac (ECL) and was described in ref. [7]. The second option is the triple-spoke linac (TSL) which is based on triple-spoke resonators (TSR) in the high- $\beta$  section of the linac [8]. As was mentioned in ref. [8] the obvious advantage of the TSL option is a significantly larger longitudinal acceptance compared to the ECL option. Since the last reports, both linac designs have been further optimized and improved. The following main modifications have been introduced: a) The peak surface electric field in all drift-tube SC resonators is assumed to be 20 MV/m, except for the first seven 4-gap quarter-wave resonators, where 16 MV/m is used. In the high- $\beta$  section the assumed peak surface field is 27.5 MV/m; b) The accelerating lattice and the phase setting of the resonators were optimized to minimize the effective emittance of the multi-q beam at the location of the strippers. Careful beam matching has been provided for

\* Work supported by the U.S. Department of Energy, Office of Nuclear Physics, under Contract No. W-31-109-ENG-38.

#ostroumov@phy.anl.gov

multi-q uranium beam; c) In the ECL design, the lattice of the high- $\beta$  section has been modified to increase the longitudinal acceptance; d) The focusing field of SC solenoids has been restricted to 9 Tesla to reduce the linac cost.

Both driver-linac designs have been optimized for simultaneous acceleration of two charge states ( $28^+$  and  $29^+$ ) in the front-end and the first section of the linac up to the first stripper, five charge states between the two strippers (average charge state is  $74^+$ ) and five charge states in the high- $\beta$  section (average charge state is  $88^+$ ).

Detailed design, optimization and simulation of the front-end is extremely important to produce a realistic six-dimensional phase space beam distribution at the entrance of the SC linac. The simulation by TRACK includes transport in the LEBT of multi-component ion beams from the ECR to the MHB, bunching and acceleration in the RFQ, and transport in the MEBT to the entrance of the SC linac. Fig. 1 presents the density distribution of the dual charge-state uranium beam in the longitudinal phase space at the front-end exit and shows the fraction of particles  $1-N/N_0$  outside a given longitudinal emittance. Simulations of larger numbers of particles reveal an increased beam halo. The MHB forms an extremely low longitudinal emittance of  $1.6 \pi$  keV/u-nsec containing 99% of particles. As seen in Fig. 1 the total emittance for 100% of all accelerated particles depends on the number of simulated particles, and could reach  $8 \pi$  keV/u-nsec for one million particles.

In the simulations, we distinguish two type of errors: static and dynamic. Misalignments of accelerator elements are considered as static errors and are generated using uniform distributions. Jitter of RF and focusing fields are examples of dynamic errors. In a real machine the effect of static errors can be partially corrected using beam measurements. The TRACK code simulates automatic steering of the multiple-charge-state beam position along the linac assuming beam position monitors feedback [9].

The particle distribution at the front-end exit has been used as the initial distribution for the simulation of the whole SC linac. Table 1 lists the values of misalignments

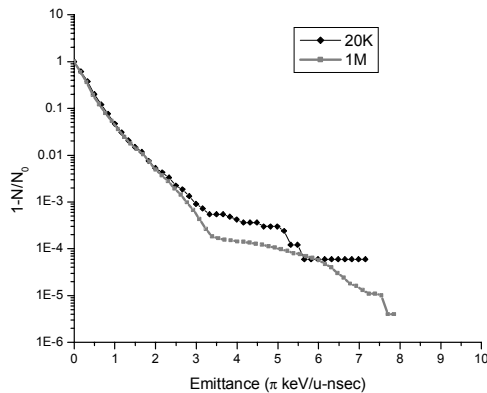


Figure 1: Fraction of particles outside of a given longitudinal emittance as a function of the emittance obtained from the simulation of  $2 \cdot 10^4$  and  $1 \cdot 10^6$  particles.

Table 1: Sources of static errors and their typical values. For solenoid displacements, the error depends on the solenoid length.

	Description	Value
1	Cavity end displacement	0.05 cm
2	Solenoid end displacement	0.015-0.05 cm
3	Quadrupole end displacement	0.01 cm
4	Multipole rotation	2 mrad

Table 2: Combinations of RF field amplitude, phase errors and foil thickness fluctuations. Uncontrolled beam losses are given for the ECL and TSL options of the driver linac.

Comb.	RF errors	Thick. fluct.	ECL	TSL
1	0.3%, 0.3°	5%	$3.0 \times 10^{-8}$	0.
2	0.3%, 0.3°	10%	$8.2 \times 10^{-7}$	0.
3	0.5%, 0.5°	5%	$5.5 \times 10^{-5}$	0.
4	0.5%, 0.5°	10%	$2.7 \times 10^{-4}$	0.
5	0.7%, 0.7°	5%	$1.4 \times 10^{-3}$	0.
6	0.7%, 0.7°	10%	$2.6 \times 10^{-3}$	0.

used in the simulations. For jitter errors and stripper-thickness fluctuations, we simulated six different combinations. They are presented in Table 2 and are generated using Gaussian distributions truncated at  $\pm 3\sigma$ , where  $\sigma$  is the rms value. The stripper thickness fluctuations are truncated at  $\pm(\text{FWHM})$ . For each error combination we simulated 200 sets of randomly generated errors. The typical number of simulated particles was  $2 \cdot 10^5$  for each error set, making a total of 40 million particles.

Figure 2 shows phase space plots at the exit of the accelerator for the different error combinations given in Table 2. From these plots, we notice that while the beam transverse size stays unchanged for the triple-spoke design it increases for the baseline design, signaling a growth in the transverse emittance which follows the growing longitudinal emittance. This may be due to a coupling of the transverse and longitudinal motion for particles near the separatrix in the longitudinal phase space. Some of these particles may lose their stability and eventually be lost. Table 2 also shows the fraction of beam lost in the high- $\beta$  sections of the linac for the different error combinations for both accelerator designs. These values are the average over the 200 sets of errors for each combination. No losses are observed in the low- and medium- $\beta$  sections of either linac. Beam losses are observed in the high- $\beta$  section for the baseline design whereas no losses are observed for the triple-spoke design. The losses increase with both the RF errors and the fluctuation in the stripper thickness. Keeping stripper-thickness fluctuations at 5% FWHM (combinations 3 and 5) and increasing the RF errors from (0.5%, 0.5°) to (0.7%, 0.7°) leads to more losses in the high energy

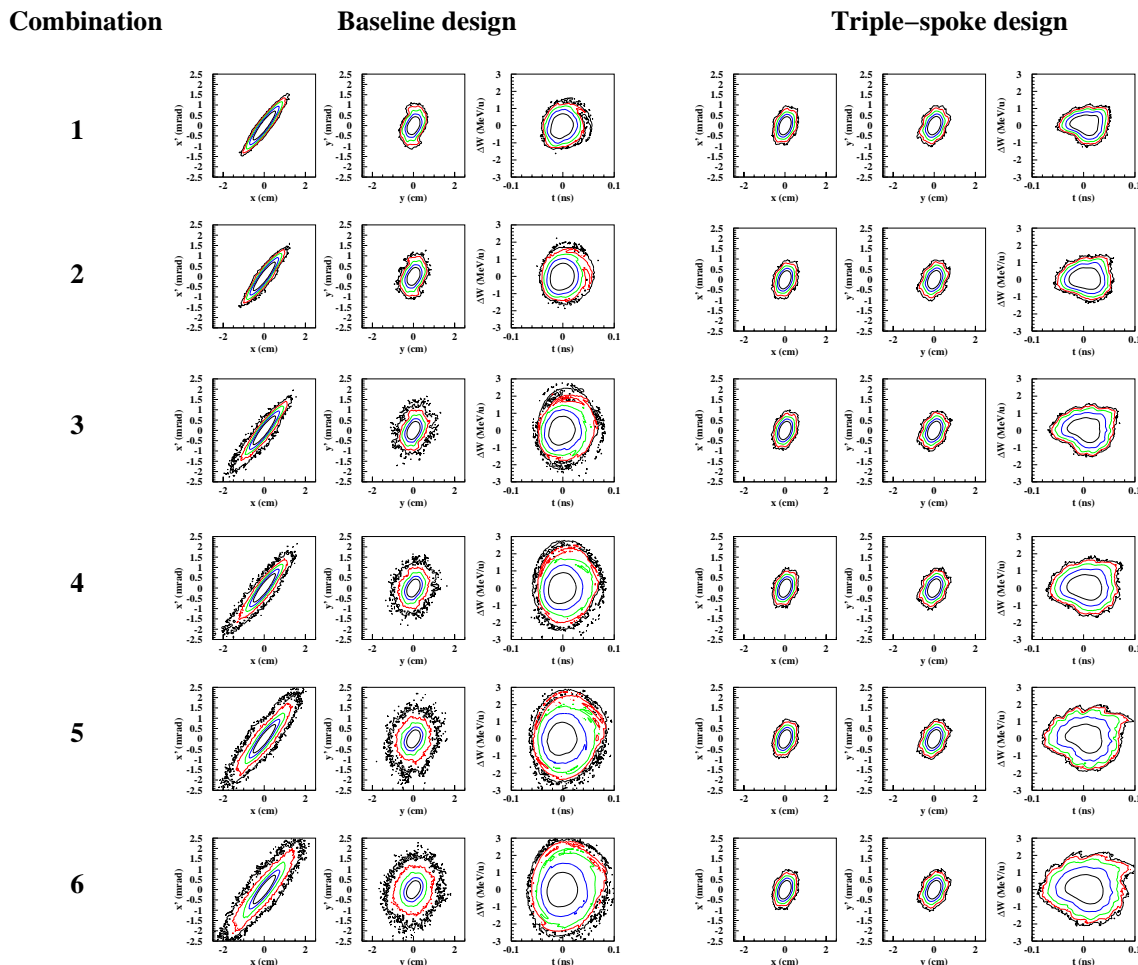


Figure 2: Phase space plots for the different error combinations of table 2. The logarithmic density isolines are represented by different colors. The outermost line and dots correspond to  $3 \cdot 10^{-8}$  level.

section than increasing the thickness fluctuations from 5% FWHM to 10% FWHM (combinations 3 and 4) while keeping the RF errors at (0.5%, 0.5°). This signals a more severe beam-halo formation for RF errors than for stripper thickness fluctuations. RF errors should therefore be kept as small as possible. Thickness fluctuations should also be limited to about 5% FWHM or less in the baseline design.

## CONCLUSION

After the finalization of the linac design, massive multi-processor simulations including misalignments of focusing and accelerating elements, random errors of the RF fields and thickness fluctuation of the stripping films have been carried out. Beam losses have been studied for two options of the RIA driver linac. The first option is based on the elliptical-cell linac (ECL) and the second option is the triple-spoke linac (TSL). The main sources of beam-halo formation are RF-field errors and beam-energy spread caused by the stripping films. Some particles become first unstable in the longitudinal phase space and eventually hit the aperture due to the loss of transverse stability. The studies show that the ECL design has more limitations concerning beam losses. RF amplitude and phase errors should be kept below 0.5%

and 0.5°. In addition, thickness fluctuations in the strippers should also be limited to less than 5% FWHM. Losses in the ECL are extremely sensitive to the longitudinal tuning of the linac. Careful phase setting to produce the lowest possible effective emittance at the stripper locations is necessary.

The triple-spoke design is more error-tolerant, displaying no uncontrolled beam losses for a wide range of RF errors, stripper thickness fluctuations, and the overall longitudinal tuning of the linac.

## REFERENCES

- [1] P.N. Ostroumov and K.W. Shepard, PRST-AB 11, 030101 (2001).
- [2] The Jazz Cluster, <http://www.lcrcl.gov/jazz>.
- [3] S. Kowalsky and H.A. Enge, RAYTRACE, MIT Report, Cambridge, Massachusetts, July 1, 1987.
- [4] V.A. Moiseev and P.N. Ostroumov, EPAC-1998, p.1216.
- [5] J.F. Ziegler, et al. The code SRIM [www.srim.org](http://www.srim.org).
- [6] B. Mustapha, et al., to be submitted to NIM.
- [7] P.N. Ostroumov. PRST-AB, 5 (2002) 030101.
- [8] K.W. Shepard, et al, PRST-AB, 6 (2003) 080101.
- [9] E.S. Lessner and P.N. Ostroumov, PAC2003, p. 3467.